Available online at www.sciencedirect.com

ScienceDirect

Physics Procedia 83 (2016) 1357 – 1366

Physics Procedia

9th International Conference on Photonic Technologies - LANE 2016

Hardness simulation of over-tempered area during laser hardening treatment

Silvia Martínez[a,*], Dmytro Lesyk[b], Aitzol Lamikiz[a], Eneko Ukar[a], Vitaliy Dzhemelinsky[b]

[a]*University of the Basque Country (UPV/EHU), Department of Mechanical Engineering, Alameda Urquijo s/n, 48013 Bilbao, Spain*
[b]*National Technical University of Ukraine (KPI), Department of Laser Physics and Applied Technologies,37 Peremohy Ave., UA-03056 Kyiv, Ukraine*

Abstract

The main problem of laser hardening process is the over-tempered structure with a hardness decrement zone in the overlapped area between different laser tracks, which may not meet the minimum hardness requirements. The over-tempered structure is located at the middle of two overlapped laser tracks or between the beginning and the ending of a closed trajectory.
In this paper, the hardness in the overlapped zones is studied by means of numerical simulations and experimental tests during a temperature controlled laser hardening with scanning optics process. Thus, in order to study their difference and to validate the proposed methodology, two steels with very different tempering curves has been used; a cold work tool steel and a medium-carbon low-alloy steel.

Peer-review under responsibility of the Bayerisches Laserzentrum GmbH

Keywords: Simulation; Hardness; Laser hardening; Over-tempered

* Corresponding author. Tel.: +34-94-601-7347; fax: +34-94-601-4215 .
E-mail address: silvia.martinez@ehu.eus

Peer-review under responsibility of the Bayerisches Laserzentrum GmbH
doi:10.1016/j.phpro.2016.08.143

Nomenclature

J_P	Hollomon-Jaffe parameter
JMA	Johnson-Melh-Avrami
TTT	temperature-time-transformation curve
PID	Proportional-Integral-Derivative control
H_p	pearlite hardness
H_f	ferrite hardness
H_m	martensite hardness
f_p	pearlite fraction
f_f	ferrite fraction
$f_{a\text{-}m}$	austenite-martensite fraction

1. Introduction

Laser hardening is a surface hardening treatment that is becoming a known manufacturing process in different industrial sectors such as the automotive industry or in the manufacture of die and molds sector. Comparing laser hardening technology with more traditional hardening processes, such as an induction or a flame hardening, it is possible to process 3D complex shapes with a minimum heat affected zone and thermal distortions. This process is being used in the industry mainly for hardening stamping dies and molds and it is also being used in long series of automotive components such us door hinges, Poprawe (2011). In addition, the interest of this process lies in the possibility of direct integration of a laser heat source on the production line without an additional quenching medium, as well as the possibility to produce different microstructures in the part with a very accurate control between the treated areas, getting a soft core with a hardened surface layer with compressive residual stresses in the surface, Bhadeshia (2012).

Furthermore, when the laser power is not high enough to reach to the hardening temperatures in the needed track width or it is a closed laser trajectory, there is an overlapped hardened zone with an over-tempered area near it. The different zones in the part after laser hardening process with multi-tracks trajectories are shown in Fig. 1. The main problem of multi-track laser hardening process is the overlapped area between different laser tracks. In this area an over-tempered structure with a lower hardness is created. The hardness values in the tempered zone may not meet the minimum hardness requirements. That over-tempered structure is located at the middle of two overlapped laser tracks or between the beginning and the ending of a closed trajectory.

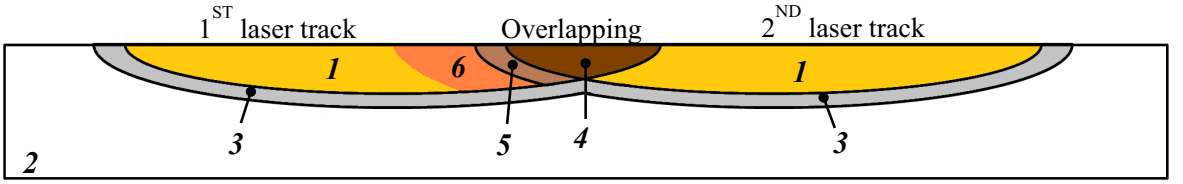

Fig. 1. (1) Hardened zone; (2) Base material; (3) Partial hardened zone; (4) Re-hardened zone; (5) Over-tempered and partial re-hardened zone; (6) Tempered-zone.

Thus, in this paper, the hardness in the overlapped zones is studied by means of numerical simulations and experimental tests during a temperature controlled laser hardening with scanning optics process. First, the numerical model developed with phase transformations during heating is explained. Then, the unknown parameters are taken experimentally for a correct hardness modelling and the results are compared with the ones obtained experimentally for different overlapped areas.

To conclude, the steels used during the experiments to study the proposed methodology and the hardness in the overlapped area, are of two types with very different tempering curves; a cold work tool steel, DIN X135CrMoV12,

and a medium-carbon low-alloy steel, DIN Ck45. The explanation of the method has been performed with DIN Ck45 carbon steel and, in Section 5, the results are compared with the ones taken from DIN X135CrMoV12 tool-steel.

2. Empirical-Numerical method

The results of the model are to evaluate and predict the hardness value in the over-tempered area between two overlapped laser tracks during laser hardening process, the process has been simulated by means of a numerical model which is summarized in the following points:

- The relationship between temperature-time-position-material phases is taken into account throughout the whole simulation.
- Numerical model is programed with a matrix based method in Matlab® software.
- The main equation programed is the heat conduction equation discretized by finite difference method.
- Temperature dependent material parameters are introduced, as density and diffusivity.
- Phase transformations are introduced during heating, Section 2.1. Phase transformations parameters are obtained previously by means of experimental tests.
- Constant temperature in the part surface during the simulation is implemented by a temperature control loop. The same PID control as the one implemented in the machine during the hardening process. It is not necessary to introduce the unknown and variable material emissivity or/and laser losses.

The results of the model are, in each simulated node of the part, the temperature and the percentage of each phase (pearlite, ferrite and austenite/martensite) along the time. During the cooling stage, it is supposed that all the austenite after a fast cooling have been converted into martensite. After the simulation, with the phase percentages and evaluating Equation 4, the hardness value in each node of the part is taken. Thus, to evaluate the hardness of the first track after treatment of the second track in the overlapped area the method explained in Section 2.2 is used. In Fig. 2 the results of the simulated hardness in a single track and in the overlapped area are shown.

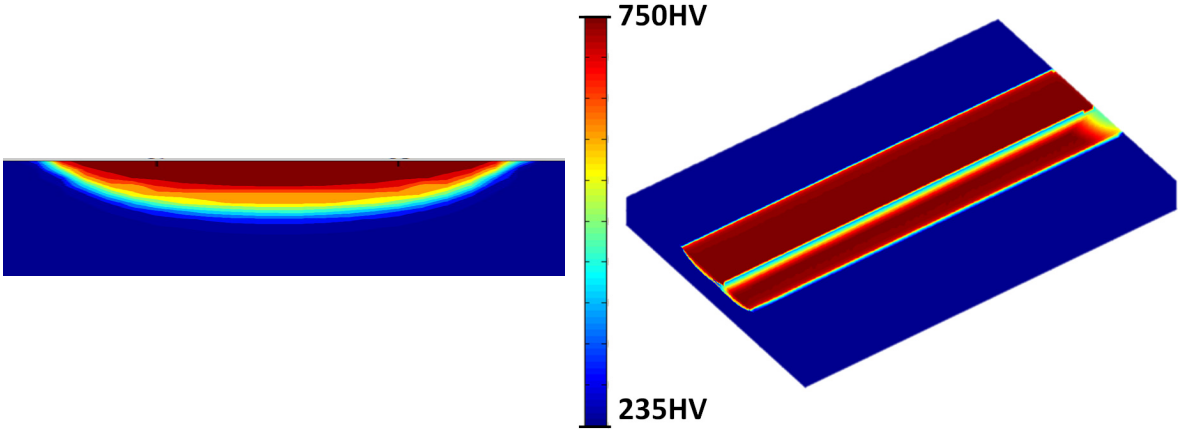

Fig. 2. (a) Hardness evolution during a single laser track; (b) Simulated hardness in the overlapped area.

The following paragraphs explain the equations programed in the model to predict the part final hardness and the parameters previous adjustment via experimental results. To show the parameters adjustment medium-carbon low-alloy steel, DIN Ck45, has been used. First, there are the Avrami equations for diffusive phase transformation during heating. Then, there is the Hollomon-Jaffe equation to predict the tempered and over-tempered hardness in the hardened area after the second laser track. Both equations are time and temperature dependent.

2.1. Avrami equations for diffusive phase transformation during a non-continuous heating

The kinetic equation of Johnson-Melh-Avrami, JMA, is used to model diffusive transformations during heating, Zhang et al. (2002). The JMA expression is presented in Equation 1 and represents the fraction of transformed material over the time in isothermal conditions.

$$f(t) = 1 - \exp\left\{-\left[k(T).t\right]^n\right\} \rightarrow k(T) = k_0 \exp\left(-\frac{Q}{RT}\right) \tag{1}$$

Where, n is a constant that depends on the nucleation mechanism and grain growth, k_0 is the pre-exponential factor related to the grain growth rate, Q is the activation energy of transformation, R the universal constant for ideal gas, T is the temperature and t is the time.

To model non isothermal conditions the fraction of transformed material balance is done in differential time steps. Thus, Equation 2 represents the fraction of transformed material for a number of subintervals that can be considered isothermal, Elmer et al. 2003. With these equations implemented in a numerical model the phase percent of transformed material can be known throughout the simulation time steps and positions in the part.

$$f_i = 1 - \exp\left\{-\left[k_0 \exp\left(-\frac{Q}{RT_i}\right)\left(\Delta t + \tau_i\right)\right]^n\right\} \rightarrow \tau_i = \frac{\sqrt[n]{-\ln\left(1 - f_{i-1}\right)}}{k_0 \exp\left(-\frac{Q}{RT_i}\right)} \tag{2}$$

Where, T_i is the temperature at the beginning of step i, Δt represents the time spent in the interval and time constant τ_i associates transformed volume fraction in step i-1, with the time that would take the material at T_i temperature to achieve the same extent of transformation.

During continuous heating the phase transformation between pearlite and ferrite to austenite is clearly shown in the dilatometry curves, Oliveira et al. (2017), or during the temperature measurement in different laser pulses, Martinez et al. (2012), as it is shown in Fig. 3.

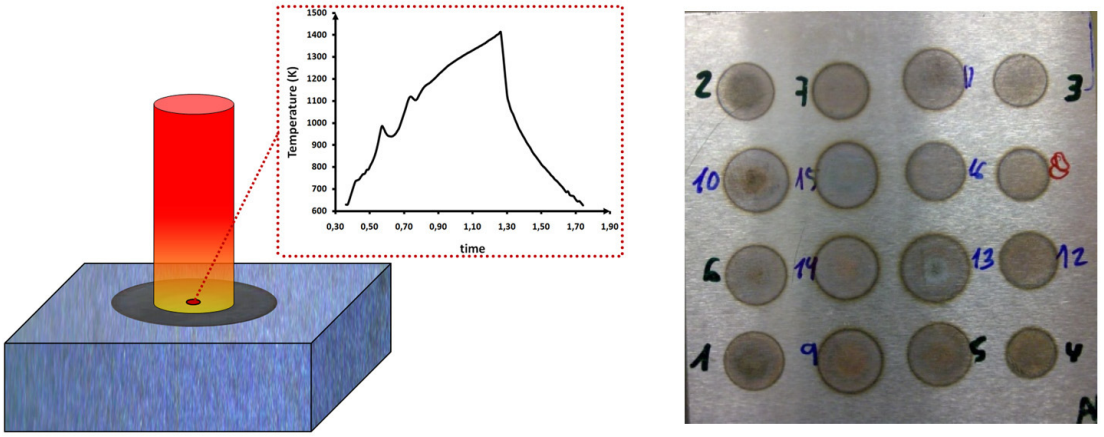

Fig. 3. (a) Diagram of temperature evolution during a single laser pulse; (b) Laser pulses at different heating rates.

The temperature measurement of laser pulses at different heating rates, similar to the heating rates during laser hardening process, has been used to the experimental acquisition of JMA parameters in the phase transformations

during heating. The results in DIN Ck45 from pearlite to austenite and ferrite to austenite temperature-time-transformations curves, TTT, are shown in Fig. 4. Hence, the pearlite to austenite transformation is narrower and faster than the ferrite to austenite one.

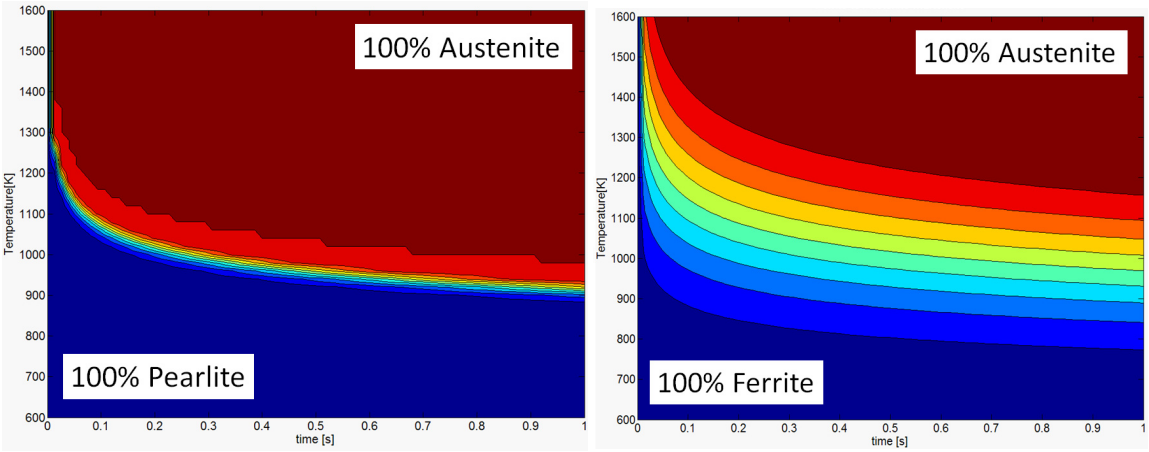

Fig. 4. (a) Pearlite to austenite TTT heating curve for DIN Ck45; (b) Ferrite to austenite TTT heating curve for DIN Ck45.

2.2. Hollomon-Jaffe parameter for hardness value after tempering

The Hollomon-Jaffe parameter, J_P, describes the effect of a heat treatment at a particular temperature for a certain time. It is used to compare the response of steel to a tempering treatment by describing an equivalence of time and temperature for thermally activated processes, Brooks (1996). The hardness after the tempering treatment depends on its temperature and its time. Thus, the same effect can be achieved with a low temperature and a long holding time, or with a higher temperature and a short holding time. This exchangeability of time and temperature can be described by Equation 3.

$$J_P = \frac{T}{1000}.\left(C + \log\left(t\right)\right) \tag{3}$$

Where T is the absolute temperature in Kelvin, C is a constant different for each material, and t is the time in hours for an isothermal condition.

In Table 1it is represented the tempering hardness and J_p parameter for DIN Ck45 steel. The different values have been obtained from material tempering tables, from material datasheets at Thyrodur (2016), and evaluating the Equation 3.

In this case, it has been assumed that there is a direct equivalence between the J_p parameter and the final hardness in the martensite structure. Hence, to evaluate the J_p parameter with the model in different points of the parts, the maximum temperature value achieved in each part point is introduce in Equation 3 with the equivalent time of 0.125s.

Table 1. Tempering curve and J_P parameter for DIN Ck45, Thyrodur (2016).

Temperature ºC/K	J_P (C=18; 1 hour)	Hardness (HV)
50 ºC/293K	5.814	750
100 ºC/373K	6.714	615
125 ºC/398K	7.164	595
150 ºC/423K	7.614	579
200 ºC/473K	8.514	545
250 ºC/523K	9.414	498
300 ºC/573K	10.314	451

3. Experimental set-up

The laser hardening tests have been performed in a machine tool specially designed for laser material processing testing. The machine is a converted 5 axes machining center with a workspace in X, Y, Z respectively of 700 x 400 x 600 mm3 and two rotary axes, B and C. The spindle has been replaced by a 2D scanner that can scan an area of 120 x 120 mm^2, which adds two additional linear axes, U and V. The laser system is a solid state fiber laser Rofin-Sinar FL010 with a maximum power of 1 kW, coupled to a 100 microns fiber connected to the scanner.

In addition, a temperature control loop to maintain the temperature constant on the surface during laser hardening process has been added as is shown in Fig. 5. The temperature during the process is measured without contact with a 2-color-pyrometer that gives the actual value of the temperature without introduce part emissivity. Then, the temperature of the part surface is stored in a computer and compared with the reference temperature. The error in temperature is used as input value for a digital PID control that adjusts and obtains an error on laser power. That power variation is added to the previous cycle value and is sent to the laser generator. Thus, a laser beam with the required power is guided by a fiber to the scanner. The scanner moves the laser beam to the corresponding point in the part surface heating it and the temperature control loop is closed.

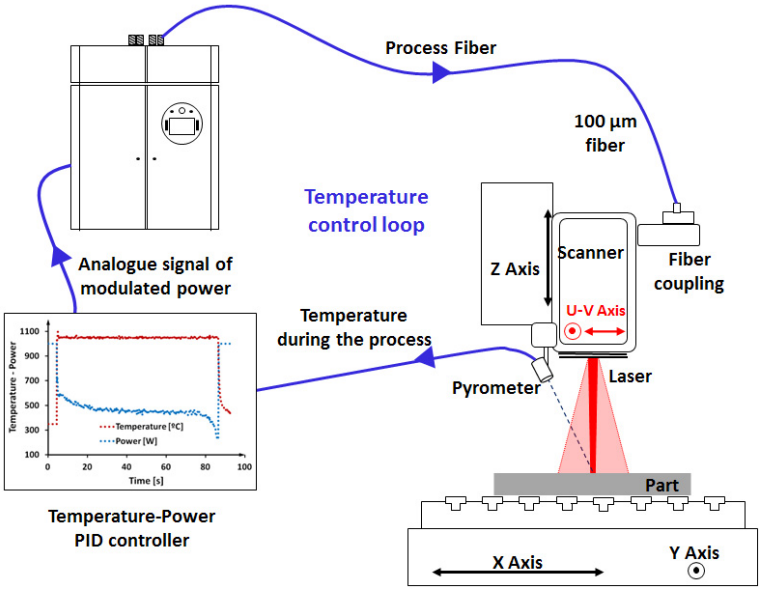

Fig. 5. Diagram of the temperature control and machine elements for laser hardening process.

On the other hand, the laser and machine parameters used during the experiments are the ones shown in the Table 2. and, more particularly, the process studied is laser hardening with scanning optics process, Martínez et al. (2016).

Table 2. Laser and machine parameters.

Parameter	Value *units*
Laser power	Variable with temperature control *W*
Laser beam diameter	1.2 *mm*
Control temperature	1100 *ºC*
Machine feed rate	120 *mm/min*
Scanning speed	1000 *mm/s*
Laser track width	10 *mm*
Overlapped area	10-25-40 *%*

4. Hardness results

In DIN Ck45 steel, the final hardness achieved in each point of the part, Equation 4, is the addition of the hardness of each phase (pearlite, ferrite and/or martensite) by the fraction of each phase in the point evaluated after the laser hardening process. Because of a rapid cooling, the same percentage of martensite than the percentage of austenite is supposed.

$$H = H_f.f_f + H_p f_p + H_m.f_{a-m} \tag{4}$$

The ferrite hardness, H_f = 95 HV, and the pearlite hardness, H_p = 282 HV, are supposed constant throughout the experiment. The martensite hardness, H_m, is supposed 750 HV in a single laser track and the value obtained in Table 1 for the same J_p parameter in the tempered and over-tempered zone in the overlapped area.

On the other hand, the initial fraction of martensite, $f_{a\text{-}m}$, ferrite, f_f, and pearlite, f_p, is 0, 0.25 and 0.75 respectively. The final fractions depend on the percentage of phase transformed obtained by the equations developed in Section 2.1.

4.1. Single laser track

The results of hardness in depth modeled in a single laser track and the ones measured in the experiments are shown in Fig. 6. Additionally, the f_p, f_f and $f_{a\text{-}m}$ in depth obtained in the model with experimental acquisition of the JMA parameters are shown in the figure. Thus, the model predicts the hardness during laser hardening process. These results are the effect of two factors; the implementation of a temperature control loop in the model to maintain it constant as during the process, and the good fit between the JMA parameters obtained by means of laser pulses and the real ones.

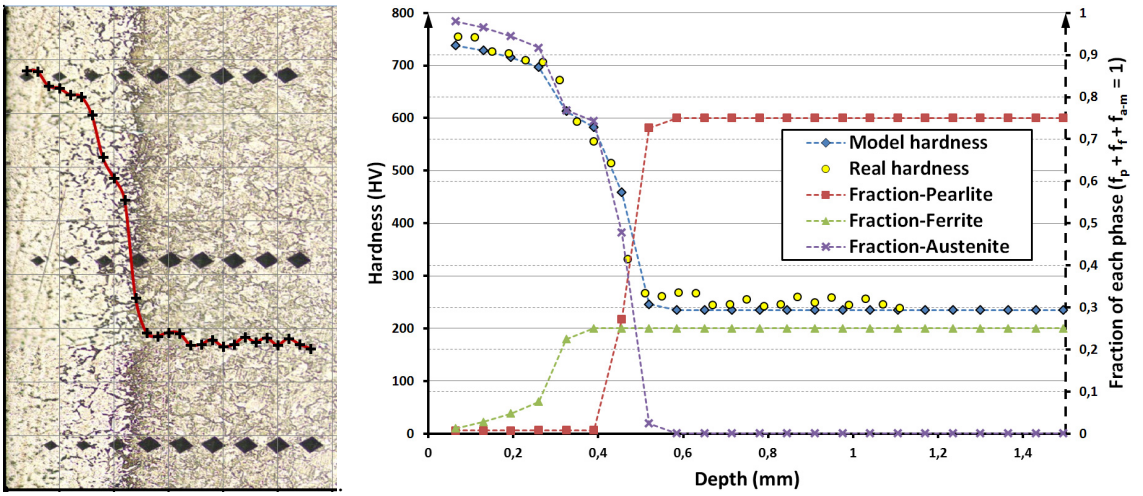

Fig. 6. Results of hardness and fraction of each phase in depth during single laser track, DIN Ck45.

4.2. Overlapped tracks (Hardened and tempered)

The results of hardness along the two laser tracks near the hardened surface, 150 μm below the surface, and with 10 % of overlapped area are shown in Figure 7. The hardness value decreases from 750 HV to near 350 HV in the over-tempered zone.

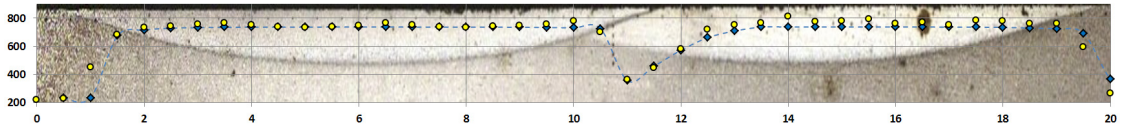

Fig. 7. Model and real hardness in 10% overlapped area, DIN Ck45.

The good adjustment between simulated and real hardness does not meet the process specifications in the over-tempering area between both laser tracks. The hardness decrement is shown in all the overlapped considered, in Fig. 8 the overlapped area is the 40% and the tempering results are similar. Thus, with DIN Ck45 this material, the difference between the real and model hardness is due to the error committed during the hardness measurements.

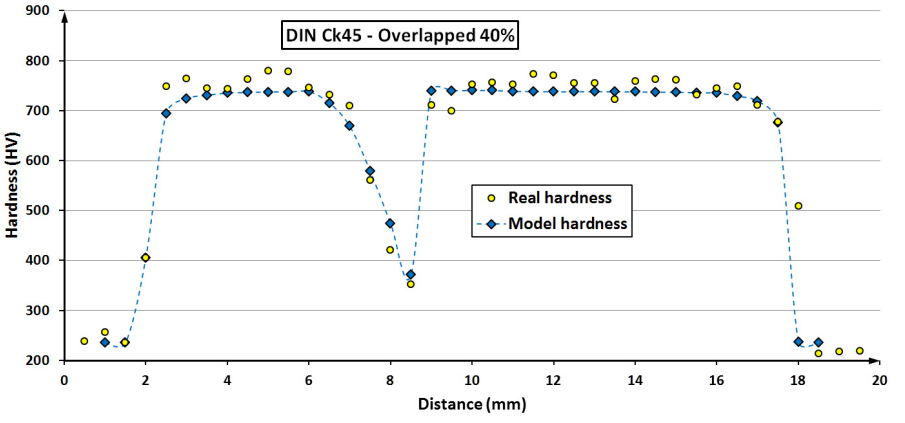

Fig. 8. Model and real hardness in 40% overlapped area, DIN Ck45.

5. Hardness results in DIN X135CrMoV12, a cold work tool-steel

The same methodology, as the one discussed in the previous sections of this article, has been used to evaluate the tempering zone in DIN X135CrMoV12 tool-steel.

During the tempering curve of DIN X135CrMoV12 tool steel there is a secondary hardness at high tempering temperatures where the hardness is increased. In this steel the tempering curve is the sum of three factors, as it is shown in the material datasheets, Thyrodur (2016): the martensite tempering curve, the hardness increment during the carbides precipitation and, finally, the transformation of retained austenite to martensite. Instead, the tempering curve of DIN Ck45 only has the effect of the martensite tempering. As it is shown in Fig. 9(a) the tempering curve of both materials is very different. Thus, the tool steel with a secondary hardening at high tempering temperatures shows a much better behavior at high temperature tempering.

In Fig. 9(b), the hardness results of the model and the real test have been compared. In general, it is not a very good fit between both graphs, but the hardness in the tempered zone is clearly improved. This low hardness decrement meets manufacturing specifications in the tempered zone.

With this material, the phase transformations during the heating are more complex, because there are a large amount of carbides, and they are not as defined as the ones appeared during the temperature measurements during a heating laser pulse in DIN Ck45 carbon steel, Fig. 3. Besides, the large number of carbides insides a ferrite, pearlite and retained austenite matrix causes a great variability in micro-hardness measurements.

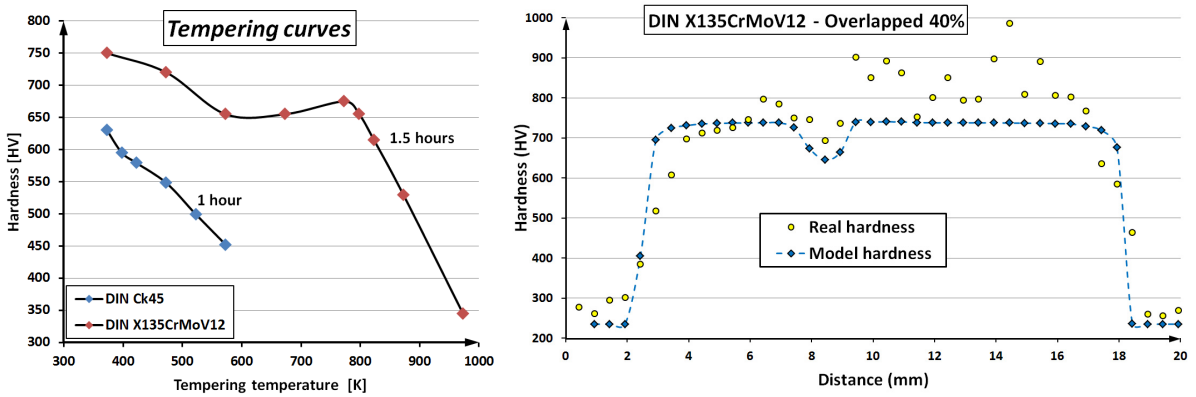

Fig. 9. (a) Differences in the tempering curves for DIN Ck45 and DIN X135CrMoV12; (b) Model and real hardness in 40% overlapped area, DIN X135CrMoV12.

6. Conclusions

In this paper the whole methodology to study the hardness in the part after multitrack laser hardening process by means of numerical simulations and experimental tests during a temperature controlled laser hardening with scanning optics process has been presented. Thus, in order to study their difference and to validate the proposed methodology, two steels with very different tempering curves has been used; a cold work tool-steel, DIN X135CrMoV12, and a medium-carbon low-alloy steel, DIN Ck45. Based on the experimental and modeled results, the following conclusions can be stated:

- The phase transformations during heating can be simulated numerically by means of JMA equation. This equation parameters have been obtained experimentally through the temperature measurement in different laser pulses.
- The final hardness achieved in each point of the part is the addition of the hardness of each phase (pearlite, ferrite and/or martensite) by the fraction of each phase in the evaluated point.

- Hardness of martensite phase after tempering can be obtained by means of Hollomon-Jaffe parameter from the tempering curves found in material datasheet.
- Laser multi-tracks with overlapping zones of 10%, 20% and 40% have been studied.
- The methodology exposed has obtained very good results in DIN Ck45 carbon steel and not too good results in DIN X135CrMoV12 tool-steel. Maybe it is due to a worse adjustment of JMA parameters and a higher error during micro-hardness measurement.
- Finally, the most important conclusion is that the tempered zone in tool steel meets the process hardness requirements, which does not happen in the studied carbon steel.

Acknowledgements

Special thanks are addressed to the Industry and Competitiveness Spanish Ministry for the support on the DPI2013-46164-C2-1-R TURBO project and RTC-2015-4194-5 AddiClean.

References

Bhadeshia, H.K.D.H., 2012. Steels for bearings. Progress in Materials Science 57, 268-437.

Brooks, C.R., 1996. Principles of the heat treatment of plain carbon and low alloy steels. (Ed.) ASM International, The materials Information Society, pp. 158.

Elmer, J.W., Palmer, T.A., Zhang, W., Wood, B., Debroy, T., 2003. Kinetic modeling of phase transformations occurring in the HAZ of C-Mn steel welds based on direct observations. Acta Materialia 51 (Issue 12), 3333-3349.

Martínez, S., Ukar, E., Lamikiz, A., Tabernero, I., 2012. Laser hardening model development based on a semi-empirical approach. International Journal of Mechatronics and Manufacturing Systems 5, 247-262.

Martínez, S., Lamikiz, A., Ukar, E., Tabernero, I., Arrizubieta, I., 2016. Control loop tuning by thermal simulation applied to the laser transformation hardening with scanning optics process. Applied Thermal Engineering 98, 49-60.

Oliveira, F.L.G., Andrade, M.S., Cota, A.B., 2007. Kinetics of austenite formation during continuous heating in a low carbon steel. Materials Characterization 58, 256-261.

Poprawe, R., 2011. Tailored Light 2 - Laser Application Technology. (Ed.) Springer.

Thyrofort. Heat treatable steels: http://www.dew-stahl.com/.

Zhang, W., Elmer, J.W., Debroy, T., 2002. Modeling and real time mapping of phases during GTA welding of 1005 steel. Materials Science and Engineering A 333, pp. 320-335.